THE PROBLEM OF INDUCTIVE INTERFERENCE BETWEEN CURRENT AND MEASURING LINES DURING ELECTRICAL SOUNDING MEASUREMENTS

Dr. Abbas Mohammed Abbas, NRIAG, Cairo, Egypt
Alexey Bobachev, MSU, Faculty of Geology, Moscow, Russia
Dr. Alexandr Karinski, IMP, Mexico City, Mexico
Dr. Vladimir Shevnin, IMP, Mexico City, Mexico

Abstract

Vertical electrical sounding (VES) is rather simple and very popular geophysical method with wide spectrum of application for the investigation of shallow depth hydrogeological, engineering geological and environmental problems. During the last few years, the VES method has been transformed into a very powerful technology called electrical imaging or electrical resistivity tomography (ERT). During the measurement of electrical signals in the field, some inductive problems can arise and produce distortions, which sometimes can spoil the data obtained. To obtain the great amount of data required for ERT, pulsed current with short impulses (0.5-2 sec) is used. Such current is very close to AC. An example of field data which was highly distorted at large separations was the main reason for conducting this investigation. In this report the origin of induction is considered. This inductive interference is more pronounced in the case of low ground resistivity. Calculations for Schlumberger and dipole axial arrays were made. Criteria for checking for inductive interference are formulated. Knowledge of this phenomenon can help in avoiding distortions and acquiring high quality field data. Some other sources of interference are also discussed.

Introduction

Geophysicists in many countries most commonly use DC instruments for resistivity survey, while in Russia low frequency AC instruments are traditionally used. But nowadays DC is really pulsed DC. A generator pulses current with + and – polarity and the measuring unit registers the voltage for each pulse and then averages these results. Pulsed DC current is really also AC, but its influence is not as well known as that of sinusoidal form (harmonic signal). AC resistivity measurements can appreciably differ from DC resistivity measurements because of electromagnetic induction. This phenomenon is a result of eddy currents in conducting rocks and mutual induction between AB and MN lines. The effect caused by this phenomenon is generally considered to be insignificant. The performance of VES on AC current as understood from DC theory is possible as long as the differences in these fields are small. However, with an increase in frequency, decrease of resistivity, or with increasing array spacing, these differences become significant. Actually the controlling factor is a small value of the *kr* modulus (*k* is a wave number, *r* - distance). As this modulus increases, the coincidence of DC and AC fields begins to diverge.

During the past few years, the VES method has evolved into the new technology of multi-electrodic sounding or Electrical Imaging (Barker, 1981). In this technology, profile soundings are carried out, by using numerous electrodes arranged beforehand along a profile and connected with a help of multicore cable to a switch-box, which is managed by an operator or computer. This technology increases the amount of detail and is suitable for study 2D and 3D media. However it requires a much

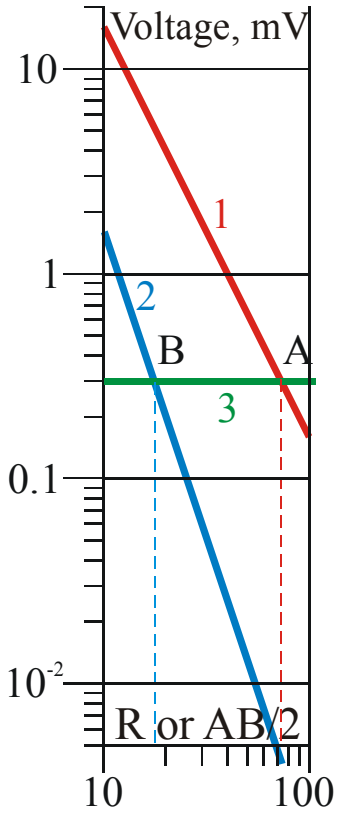

Fig.1. Signals in MN line for Schlumberger array (1), dipole axial array (2) as function of distance (for uniform earth) and supposed induction (3).

larger number of measurements. This makes it necessary to increase the speed of measurements and to use higher frequencies or shorter pulses of current than used for traditional sounding. In some cases, a dipole axial array is used. The intensity of an electrical field caused by the conducting medium for a dipole axial array is less than for Schlumberger or Wenner and it decreases faster (proportionally R^3, instead of R^2), while the inductive signal at use of multicore cable in the multi-electrodic system is probably commensurable with that for a Schlumberger array.

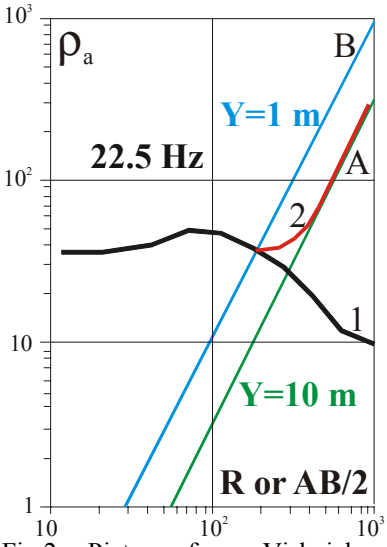

Fig.2. Picture from Vishnjakov (1967). A – inductive asymptote for Y=10 m, B – that for Y=1 m, 1 VES – DC (no distorted), 2 – VES – AC (distorted at the right part).

The influence of induction during low frequency AC measurements has mainly been considered in literature discussing low-frequency IP measurements. The IP signal is many times smaller than the resistivity signal. Many AC IP instruments were developed over 50 years ago and inductive interference was rather noticeable. That is why some techniques of induction estimation and elimination from IP data were developed. These were developed for measurements at two or three frequencies (Millett, 1967; Hohmann, 1973; Dey, and Morrison, 1973). VES uses DC or a single AC frequency. That is why techniques for canceling inductive effect from IP data are not valid for VES measurements. For many years DC was used for VES surveys, except in Russia, where AC was very popular after the 1950s. That is why Russian geophysicists published diagnostics of inductive interference on VES data first.

Vishnyakov (1967) discussed the theoretical consideration of inductive coupling for AC VES. According to Vishnjakov, inductive coupling between AB and MN lines for Schlumberger array can be described by a complex formula, which in very simplified form looks like $\rho_a = A \cdot f \cdot r^2$, where A is constant coefficient ($A=5.877 \cdot 10^{-5}$ for f=22.5 Hz and Y=1 m). Coefficient A is function of Y – the distance between AB and MN lines. Vishnjakov explained, that the signal in the MN line is actually a sum of two signals. One signal is generated by the earth and includes information about geological structure (1 or 2, fig.1) and the other one is a result of induction (line 3, fig.1). At low frequencies (several Hz) this second signal is low in comparison with the first "geological" signal. The second inductive signal is approximately the same for all distances as shown by line 3 on fig. 1 which is from Vishnjakov (1967). The geological signal becomes smaller and smaller with increasing array distance. The geological signal is inversely proportional to R^2 for Schlumberger array (line 1, fig.1) and R^3 for dipole axial array (DAA) (line 2, fig.1) above uniform halfspace, going down at the angle 63° (its tangent is equal to -2) or 71.5° (its tangent is equal to -3). That means that for small distances the geological signal is greater than the inductive signal until point A for

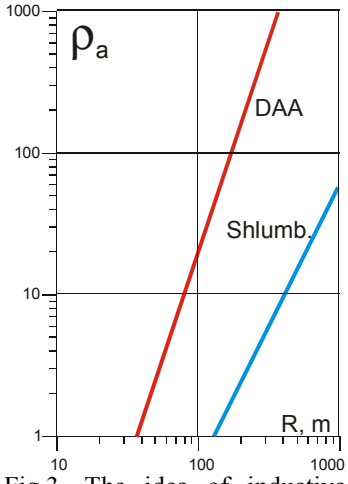

Fig.3. The idea of inductive asymptotes for AMNB and dipole axial arrays as a consequence of fig.1.

Schlumberger array or point B for DAA as shown on fig.1. At larger distances, the inductive signal is greater (after point A or B at fig.1). This inductive signal of constant amplitude multiplied by a geometrical coefficient gives an apparent resistivity curve at great distances going up at an angle whose tangent is equal to 2 for Schlumberger array or 3 (for DAA) as shown on fig.2 and 3. This part of the sounding curve is called the inductive curve. We want to note that fig.3 shows only a preliminary idea, following from fig.1. From this picture we can conclude that inductive influences on dipole data are much stronger and begin at smaller distances. This preliminary conclusion is the result of fig.1, where geological signal for DA array is lower than for Schlumberger array, while the inductive signal (in the case of multi-electrodic sounding) is the same.

Experimental sounding curves on figs.16-17 have distorted right parts, going upward at the angle 71.5°. That superficial similarity of experimental data distortions with our idea of inductive influence, displayed on figs. 1 and 3 urged us to pay more attention on inductive influence.

Theoretical problem setting

Let's develop expressions for an electromagnetic field excited by a harmonically varying (at constant frequency) rectilinear current in AB line (A, B are point electrodes on the ends of AB line), believing, that AB line lays on the horizontal surface S of a homogeneous conducting halfspace. At the conclusion of this expression it is assumed, that the source is either inside the conducting halfspace or in the air, and then dropped on the earth surface. The check has shown, that in the limit, both options yield the same result.

Let's assume, that the ground is non-magnetic, that electrical current varies synchronously at full length of cable, and also, that the conditions of quasistationary state of the electromagnetic field are valid. Let's introduce coordinates X, Y and Z. X coordinate is along profile and array direction, Y is in perpendicular direction, and Z is upward.

At first we shall define a field of a horizontal element I dl of a linear current I, located in the conducting halfspace V_1 at distance h from the boundary. Let's enter vector potential of an electrical type A connected with an electromagnetic field components (E, H) by equations.

$$\mathbf{H} = \frac{1}{\mu_0}\,\mathrm{rot}\mathbf{A}, \quad \mathbf{E} = i\omega\mathbf{A} + \frac{1}{\mu_0\sigma}\,\mathrm{grad}\,\mathrm{div}\mathbf{A}.$$

In the Cartesian coordinate system with the beginning at the center of a current element, axis X is along the current direction and axis Z is directed vertically upward along a perpendicular line to the boundary S between halfspaces V1 and V2 (with specific electrical resistivities ρ_1, ρ_2, respectively), we have:

$$\mathbf{A} = \mathbf{A}_x + \mathbf{A}_z.$$

Tangential components of an electromagnetic field are defined by expressions:

$$H_x = \frac{1}{\mu_0}\frac{\partial A_z}{\partial y},\ H_y = \frac{1}{\mu_0}\left(\frac{\partial A_x}{\partial z} - \frac{\partial A_z}{\partial x}\right),\ E_x = i\omega\left(A_x + \frac{1}{k^2}\frac{\partial}{\partial x}\mathrm{div}\mathbf{A}\right),\ E_y = \frac{i\omega}{k^2}\frac{\partial}{\partial y}\mathrm{div}\mathbf{A},$$

where $k = k_1, k_2$ - wave number of appropriate medium.

The equation for vector potential components of an element of a current in halfspaces V_1, V_2, satisfying the differential equations and conditions in the special point and in infinity, can be written in the following form:

$$A_x^{(1)} = \frac{\mu_0 Idl}{4\pi}\int_0^\infty \frac{m}{m_1}\left(e^{-m_1|z|} + Be^{m_1 z}\right)J_0(mr)\,dm, \quad A_z^{(1)} = \frac{\mu_0 Idl}{4\pi}\frac{x}{r}\int_0^\infty \frac{m}{m_1}Ce^{m_1 z}J_1(mr)\,dm,$$

$$A_x^{(2)} = \frac{\mu_0 Idl}{4\pi}\int_0^\infty \frac{m}{m_2}De^{-m_2 z}J_0(mr)\,dm, \quad A_z^{(2)} = \frac{\mu_0 Idl}{4\pi}\frac{x}{r}\int_0^\infty \frac{m}{m_2}Ge^{-m_2 z}J_1(mr)\,dm,$$

where B, C, D, G - multipliers dependent from m,

$$r = \sqrt{x^2 + y^2},\ m_{1,2} = \sqrt{m^2 - k_{1,2}^2},\ \mathrm{Re}(m_{1,2}) > 0.$$

Unknown B, C, D and G are determined, requiring continuity on S (at z=h) of tangential components of electromagnetic field.

Believing, that q is a point and $dl=dx_q$ is an element of AB line, it is simple to determine the electromagnetic field of such a line by integration. In particular, for E_x component we have:

$$E_x^{AB} = \frac{i\omega}{dl}\int_{x_B}^{x_A}(A_x + \frac{1}{k^2}\frac{\partial}{\partial x}\mathrm{div}\mathbf{A})\,dx_q = \frac{i\omega}{dl}\left(\int_{x_B}^{x_A}A_x dx_q - \frac{1}{k^2}\mathrm{div}\mathbf{A}_{x=x_A} + \frac{1}{k^2}\mathrm{div}\mathbf{A}_{x=x_B}\right). \quad (1)$$

At $h\to 0$, $z\to 0$, $\rho_2\to\infty$, $k_2\to 0$, $m_2\to m$ we receive:

$$E_x^{AB} = \frac{\rho_1 I}{2\pi}\left\{k_1^2\int_{x_B}^{x_A}\left[\int_0^\infty \frac{m}{m+m_1}J_0(mr)\,dm\right]dx_q - \frac{x_A - x}{r_A}\int_0^\infty mJ_1(mr_A)\,dm + \frac{x_B - x}{r_B}\int_0^\infty mJ_1(mr_B)\,dm\right\},$$

where

$$r_A = \sqrt{(x_A - x)^2 + y^2}, \quad r_B = \sqrt{(x_B - x)^2 + y^2}$$

Carrying out transformations using Weber and Summerfield integrals it is possible to present expression (1) in a simpler form:

$$E_x^{AB} = \frac{\rho I}{2\pi}\left\{\int_{x_B}^{x_A}\frac{1}{r^3}\left[(1-ikr)e^{ikr} - 1\right]dx_q - \frac{x_A - x}{r_A^3} + \frac{x_B - x}{r_B^3}\right\}. \quad (2)$$

If the both lines AB and MN are parallel to X axis, the EMF of electrical field is:

$$\mathcal{E}_{MN} = \int_{x_M}^{x_N} E_x dx, \quad \mathcal{E}_{MN} \approx -E_x\left(\frac{x_M + x_N}{2}, y\right)\cdot MN.$$

The second equation is true at a position of MN line near the middle of AB line, $x_M > x_N$ and MN<<AB.

In the general case we have:

$$\begin{aligned}\mathcal{E}_{MN} &= \frac{\rho I}{2\pi}\int_{x_M}^{x_N}\left\{\int_{x_B}^{x_A}\frac{1}{r^3}\left[(1-ikr)e^{ikr} - 1\right]dx_q - \frac{x_A - x}{r_A^3} + \frac{x_B - x}{r_B^3}\right\}dx = \\ &= \frac{\rho I}{2\pi}\left\{\frac{1}{r_{AM}} - \frac{1}{r_{AN}} - \frac{1}{r_{BM}} + \frac{1}{r_{BN}} + \int_{x_M}^{x_N}\int_{x_B}^{x_A}\frac{1}{r^3}\left[(1-ikr)e^{ikr} - 1\right]dx_q dx\right\},\end{aligned} \quad (3)$$

where r_{AM}, r_{AN}, r_{BM}, r_{BN} are distances between corresponding current and measuring electrodes, $r = \sqrt{(x - x_q)^2 + y^2}$, and y is the distance between *AB* and *MN* lines.

For symmetrical array *AMNB,* when *MN* << *AB* and the point of origin of the *x* coordinate is in the middle of *AB* and *MN,* from (3) we get:

$$\mathcal{E}_{MN} \approx \frac{\rho I}{\pi}r_{MN}\left\{\frac{r_{AO}}{\left(r_{AO}^2 + y^2\right)^{3/2}} + \int_0^{x_A}\frac{1}{r^3}\left[1 - (1-ikr)e^{ikr}\right]dx_q\right\}, \quad (4)$$

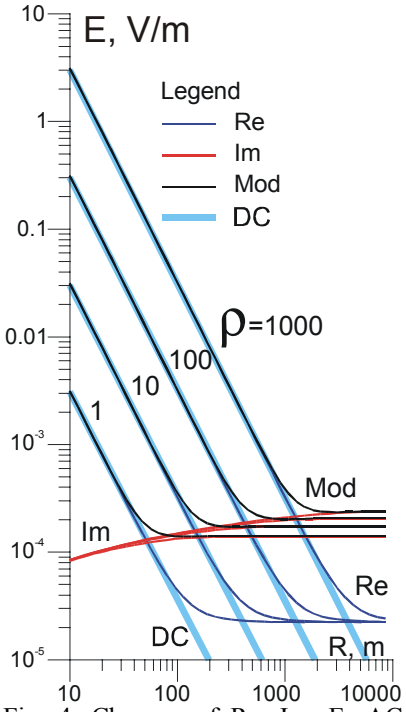

Fig. 4. Changes of Re, Im, E_x AC modulus and E_x DC from AB/2 spacing for Schlumberger array.

where $r_{AO} = r_{AB}/2$. If $r_{AO} >> y$, then from (4) we get:

$$\varepsilon_{MN} \approx \frac{\rho I}{\pi} r_{MN} \left\{ \frac{1}{r_{AO}^2} + \int_0^{x_A} \frac{1}{r^3} \left[1 - (1 - ikr) e^{ikr} \right] dx_q \right\}. \qquad (5)$$

The case of Schlumberger array

The electrical field on alternating current is a complex value and has real and imaginary parts. In practice it is possible to measure either modulus of a signal, or its real part (for example with the help of a synchronous detector in a measuring scheme).

On fig.4 the diagrams of Re, Im and modulus of Ex component of electric field are displayed depending on current electrodes' spacing AO for Schlumberger array. The calculation is executed using formula 4 for a field frequency 22.5 Hz (Vishnjakov used this frequency) and distance (parallel shift) between current and measuring lines Y=1 m. The resistivity of the background environment is 1; 10; 100 and 1000 Ohm.m and a current value in AB line = 1 A. From these results and similar accounts for other experimental parameters it is possible to make the following conclusions:

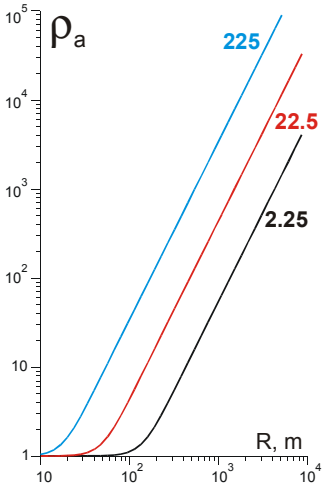

Fig. 5. Dependence of inductive asymptote's position from frequency for modulus E_x.

1. An imaginary E_x component increases slowly with spacing, and a real one sharply decreases.
2. At small spacing the imaginary component of an electric field E_x is small in comparison with a real one, but begins to exceed it with increased spacing.
3. The real AC E_x component at large spacings diverges from the model's properties, while right asymptotes of the diagrams for resistivities 1 - 1000 Ohm.m coincide.
4. The dependence of the imaginary component from ground resistivity increases with increasing spacing.
5. The modulus of a signal at small spacings is determined by the real component, and at greater spacings by the imaginary component.
6. The range of acceptability of DC approximation for real AC measurements depends on the type of measurements (modulus of a signal or real component) and coincides with the rectilinear part of the diagrams on fig.1 going down at an angle 63°. At the deviation of the curves from rectilinear paths the DC law becomes broken.
7. The inductive signal does not change with increased distance (at Re E_x measurements) or changes very little (at modulus measurements).

At recalculation into apparent resistivity,

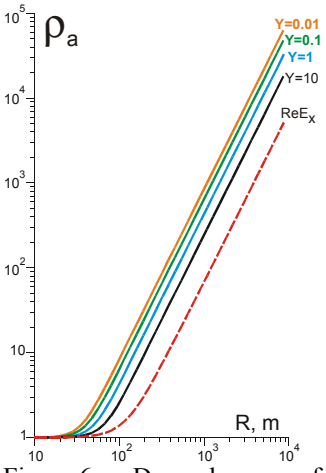

Fig. 6. Dependence of inductive asymptote's position from Y for modulus and ReE_x.

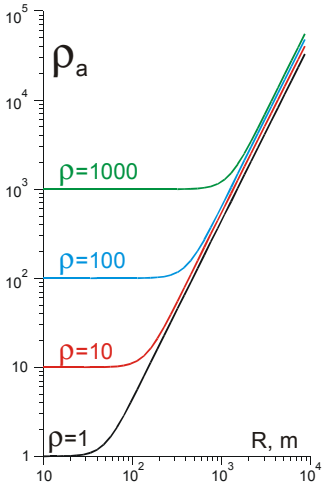

Fig.7. Dependence of inductive asymptote's position from halfspace resistivity for modulus E_x.

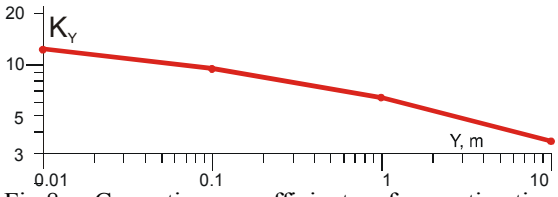

Fig.8. Correction coefficients for estimation inductive asymptote position from ReE_x for E_x modulus.

VES curves for a homogeneous halfspace will look like those on fig. 2 and figs. 5-7. At small spacings, VES curves are going horizontally at a level ρ_1, then on longer spacings go upwards at an angle about 63° (it is the so-called inductive asymptote or violation of DC law and represents the complete or partial loss of connection of ρ_a curve with the model properties). The position of the inductive asymptote most strongly depends on frequency (fig. 5).

To a lesser degree this position depends from Y (fig. 6) and from resistivity of halfspace (fig. 7). $\rho_a^{ind.as.}(Mod\ E_x) = fun(f, \rho, Y)$.

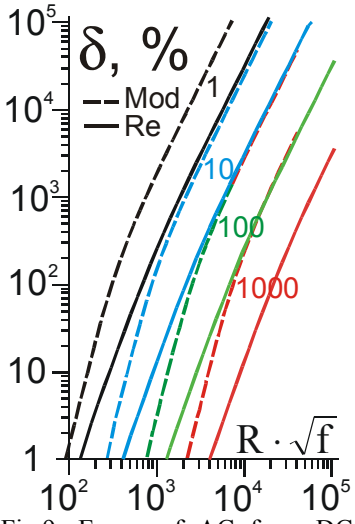

Fig.9. Errors of AC from DC apparent resistivities' deviation for Schlumberger array.

It is interesting to note, that the position of inductive asymptote when apparent resistivity is calculated on real component, measurements does not depend from Y, but only from frequency (it is shown by a dotted line on fig. 6), it is a consequence of uniform asymptote for ReE_x (fig. 4). $\rho_a^{ind.as.}(\mathrm{Re}\,E_x) = fun(f)$. This is true only for right asymptote.

Besides asymptote for ReE_x is moved from asymptote for E_x modulus to greater spacings (in 3.5 times along spacings axis or in 10 times along resistivity axis for Y=0.01), that creates additional favorable opportunities for AC VES with ReE_x measurements. The equation for ReE_x asymptote: $\rho_a = A \cdot f \cdot r^2$, where $A=3.247 \cdot 10^{-6}$. For modulus E_x measurements A' in the last formula is A K_Y (see K_Y on fig. 8). Our result for Schlumberger array is very similar to that of Vishnjakov.

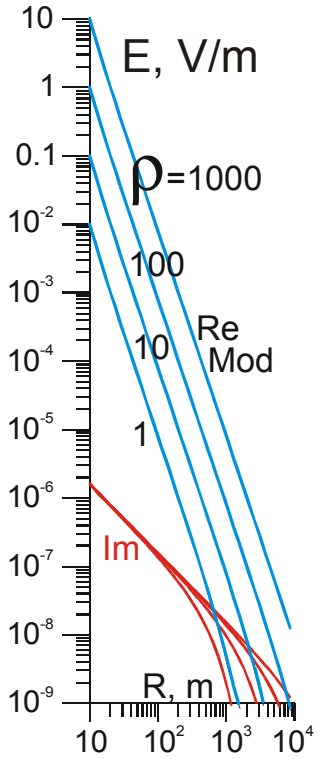

Fig. 10. Changes of Re, Im, E_x AC modulus from R spacing for dipole axial array.

The inductive influence can be estimated on VES curve's output on inductive asymptote, as shown on fig.5-7. But it is possible by taking into account conditions of experiment and the instrumental parameters to estimate the percentage value of the inductive influence. For this purpose, it is possible to transform the data, submitted on a fig.5-7 into values of error, on which apparent resistivity ρ_a differs from true resistivity ρ of the medium. In this case it is more convenient to use not array spacings along abscissa axis, but the values of its product to frequency $R\sqrt{f}$. Along vertical axis the error value or the deviation of apparent resistivity ρ_a from true resistivity ρ, calculated under the next formula: $\delta = (\rho_a - \rho_1)/\rho_1 \cdot 100\%$, is displayed. These diagrams for Schlumberger array are submitted on fig.9. Knowing resistivity of environment, working frequency and array spacing, it is possible to estimate value of a deviation from DC law in %. The continuous lines on fig.9 show errors for the real part E_x, and dotted lines - for the modulus. For E_x modulus the inductive influence is stronger and the errors are higher in 6-7 times.

Case of dipole axial array.

Accounts for dipole axial array were made on formula 3 when y=0 for operation frequency 1 Hz and AB and MN length 5 m.

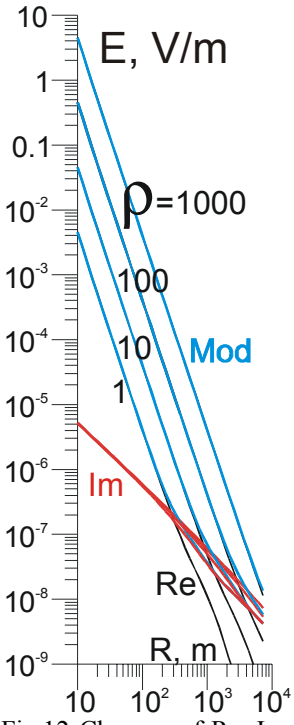

Fig.12 Changes of Re, Im, E_x AC modulus from R spacing for dipole axial array in multielectrodic system.

From fig.10 and similar accounts for dipole axial array it is possible to make the following conclusions:

1. The imaginary E_x component decreases with spacing approximately as 1/R, and a real one sharply decreases as $1/R^3$. That is different from the case of Schlumberger array.

2. On small spacing an imaginary component of an electric field Ex is at 4-7 orders of magnitude smaller then a real one, and these are comparable only at spacings more then 1000 m. The modulus of a signal at distances smaller 1000 m is practically independent from inductive influence.

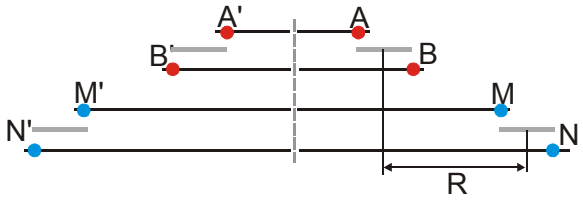

Fig. 11. Scheme of multielectrodic dipole axial array for calculation of inductive influence.

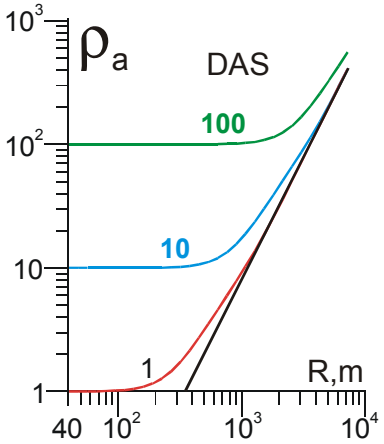

Fig.13. Inductive distortions for multielectrodic DA array at 1 Hz.

Case of dipole axial array in multielectrodic system.

For calculation of inductive influence in the case of dipole axial array in multielectrodic system (this is the case of field experiment, considered below) the artificial scheme presented on fig.11 was considered. Electrodes A, B, M, N were reflected from the boundary, marked by vertical dotted line on fig.10. All electrodes are connected to wires separated at the distance dY. The array spacing R is measured along X direction between centers of AB and MN. Length of AB and MN is 5 m. Frequency is 1 Hz. Account was made on formula 3. Results of calculation are presented on fig.12.

From fig.12 and similar accounts for dipole axial array in multielectrodic system it is possible to make the following conclusions:

1. An imaginary E_x component decreases with spacing approximately as 1/R, and a real one sharply decreases as $1/R^3$.

2. On small spacing an imaginary component of an electric field E_x is at 3 - 4 orders of magnitude smaller then a real one, and is comparable at spacings about 200 - 300 m. The amplitude of the imaginary component in multielectrodic dipole axial array is higher than in the case of traditional dipole axial array (fig.10) while the real part of electric field is nearly the same.

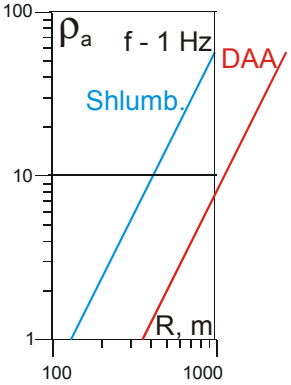

Fig.14. The position of inductive asymptotes for DAA and Schlumberger array on account result.

3. The E_x modulus on small spacings is determined by real component, and on greater spacings (R>200 m) – by imaginary component.

4. Decreasing of E_x imaginary component as 1/R resulted to appearance of ρ_a inductive asymptote going upward at angle ($1/R\ R^3 = R^2$), which tangent is 2 (fig.`13-14), not 3. The position of inductive asymptote for DAA is to the right from that for Schlumberger array, that is differ from fig.3.

On fig. 15 the diagrams of errors, similar to fig. 9 for multielectrodic dipole axial array (for a case of E_x modulus measurements) are shown. These diagrams (fig.9 and 15) are very similar both on form, and on errors' values. The important conclusion from fig. 15 is, that at medium resistivity 1 Ohm.m and frequency 1 Hz, at spacings smaller 100 m the deviations from DC law for

dipole axial array are less then 1%. That says or about incorrect account of inductive influence for multielectrodic dipole axial array or about the fact that distortions of field sounding curves (figs. 16-17) were caused by some other reasons. Such reasons are discussed below.

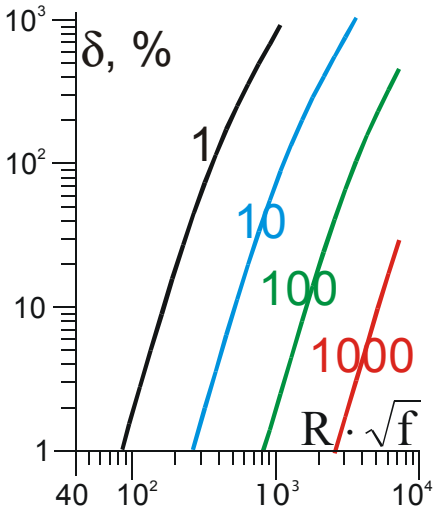

Fig.15. Errors of AC from DC apparent resistivities' deviation for DAA case.

Field data consideration

At field work in Egypt, made by National Research institute of Astronomy and Geophysics (NRIAG) with IRIS instrument Syscal R2 on pulced current at 1 Hz frequency with multi-electrodic technology and dipole axial array, electrical sounding data, represented at fig.16-17, were received. Each current pulse duration time was 500 ms. Fieldwork was made in an agricultural area. The resistivity values were very low in the range of pure clay to sandy clay, between 2-15 Ohm-m. Dipole axial array with AB and MN 5 m spacing was applied at 20 profiles. Some profiles include 20 equally spaced electrodes, while the other profiles include 40 electrodes (multi-system), which were converted into 17 or 37 separate dipole axial soundings. These 20 profiles were subdivided into group with strong inductive distortion (fig.16: Pr. 6, 7, 9, 10, 11, 16, 17) and the other group with weak distortion (fig.17: Pr. 1-21, except above-mentioned). Each profile was statistically processed for receiving median VES curve. At fig.17 distortions begin after spacing 50 m. At fig.16 some data are distorted at smaller distances 10-50 m. But angle of right part of sounding curves at fig.16 is close to 71.5°.

The situation on fig. 16 needs to be explained more. Sounding curves have distortions at different distances, and at much smaller distances than inductive asymptote for 1 Hz. And angle of sounding curves' parts going upward is closer to 71.5°, then to 63°. This is not an induction, that we proposed earlier. Probably the distortions have another origin. Really Vishnjakov (1967) and later A.V.Kulikov et al. (1985) proposed some other additional distortions' mechanisms.

Between measuring and current lines the direct interferences of two types are possible, which shortly could be named magnetic and electrical interference. The wires of measuring line with the consistently connected grounding resistances R_M, R_N and R_{input} form the closed electrical contour (fig.18, A). Variables of the magnetic field from the current line will produce in this contour electromoving force (EMF), which in basic is enclosed to the entrance of measuring unit. So arises magnetic interference between current and measuring lines. Magnetic interference has the higher intensity the greater is magnetic field, i.e. near to current line's wire. The presence of

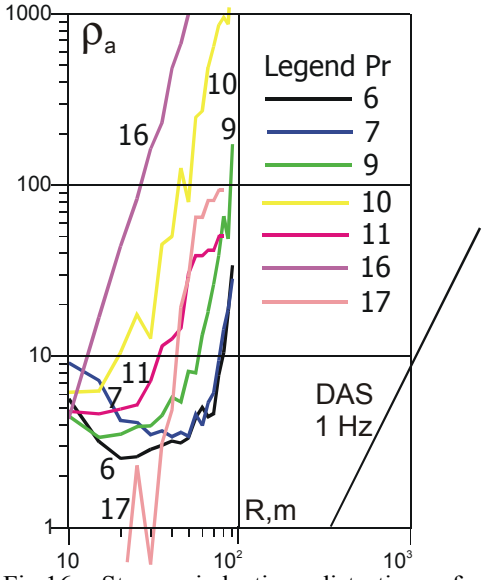

Fig.16. Strong inductive distortions for seven profiles.

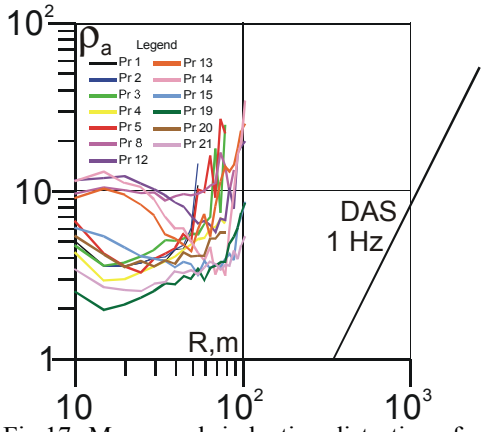

Fig.17. More weak inductive distortions for 13 profiles.

magnetic interference can be established as follows. Not changing a position of M and N grounding, change length and form of measuring wire, lying on ground surface. If thus the results of measurements do not change, magnetic interference is absent. Magnetic interference does not depend on a resistance of MN grounding.

Electrical interference arises through capacitative connection between current and measuring lines. For a signal of electrical interference a resistance of measuring unit R_{INPUT} and grounding resistance appear included parallel, and as $R_{MN} << R_{INPUT}$, the signal of electrical interference appears directly proportional to R_{MN} (fig.18, B), i.e. is connected to a resistivity of the top layer. The presence of electrical interference is established as follows. Not changing a position of M and N grounding and connecting wires it is necessary to change grounding resistivity, for example, putting deeper M and N electrodes. If after that the result of measurement does not vary, electrical (galvanic or capacitative) interference is absent.

Matushko (1999) offered one more possible reason of VES curves distortions resulted from alternating current usage. It is outflow with current line AB through capacitative connection between current wire and ground (fig.18, C). When resistances of current line grounding R_A, R_B are low, this outflow can be neglected. When grounding resistance is high, as in case of cross-section with a high specific resistivity of the top layer, the share of current, which flows down from a wire through capacitative outflow, grows. Though outflow current is small, but the places of outflow are much closer to measuring line, than current electrodes. Thus, the contribution of outflow current to a signal (measured in MN line) can be significant. What the outflow through wire capacity does exist, the application in Russia non-contact electrical resistivity survey proves. This non-contact technology is based upon capacitive current (Nahabtcev et al., 1985; Sapozhnikov, 1996).

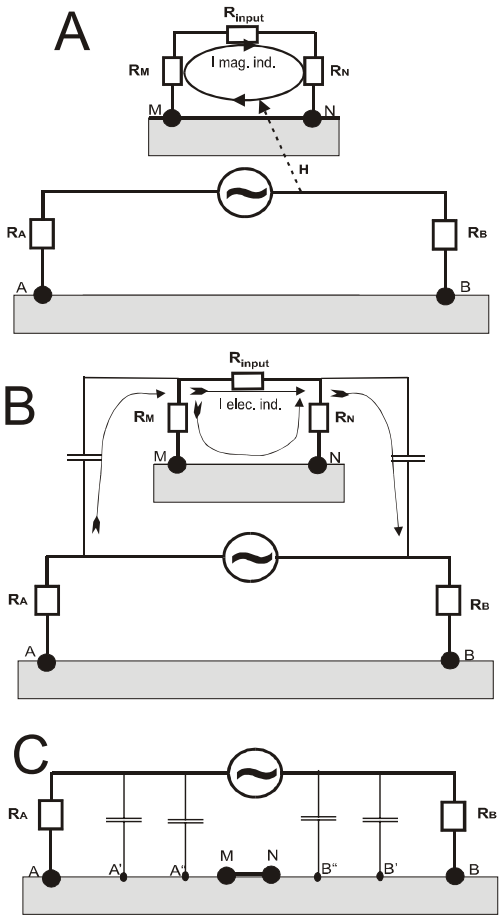

Fig.18. Three possible mechanisms of AC interactions between current and measuring lines (on Vishnjakov, Kulikov and Matushko).

For better understanding EM induction and sounding curves distortion we need new theory of distortions, caused by inductive and capacitive interactions between current and measuring lines. Wide usage of multi-electrodic sounding technology with multi-core cable for electrical resistivity tomography needs more theoretical base for high quality field measurements.

One more explanation of distorting effect is based on the next argumentation. The "geological" signal in array of dipole axial sounding is quickly descending with growth of array spacing. If we suppose that in a metering circuit a small signal of a constant amplitude is presented, which at larger electrode spacings is becoming more than "geological" signal, after multiplying to geometrical coefficient of array it will give a part of sounding curve going upward at an angle, which tangent is equal 3. Such signal can be resulted from a current leakage in multi-core cable through defects in wires' insulation or due to conducting film of moisture in the plug or not enough high resistivity of cut off electronic clues commuting current and measuring channels in multielectrodic array. To determine the real reason of the detected field data distortion the special study is necessary.

Conclusions

Usage of AC or pulsed DC in multi-electrodic sounding technology with multicore cable at low resistivity of the earth can give distortions of sounding curves and spoil field results. Features of inductive distortions are right asymptotes of sounding curves going upward at the angle, which tangent is equal 2 for dipole axial array, for Schlumberger and Wenner array.

Possibility of induction can be estimated depending on the operational frequency of the instrument. So-called DC instruments really use pulsed current, which signal can also be distorted by induction.

The most accurate criterion of the absence of inductive distortion is independence of measuring signal from frequency. For that instrument should have several frequencies or time lengths of pulses.

There is need in new theory of distortions, which take into account both inductive and capacitive interactions between current and measuring lines and the influence of grounding resistances on electrodes.

Acknowledgments

The authors would like to express their gratitude to Mexican Petroleum Institute, Department of Production Technology for support of this study.

References

1. Barker R.D. 1981. The offset system of electrical resistivity sounding and its use with a multicore cable. *Geophysical Prospecting*, 29, 128-143.
2. Dey, A. and Morrison, H. F., 1973, Electromagnetic coupling in frequency and time-domain induced-polarization surveys over a multilayered earth: *Geophysics*, v. 38, p. 380-405.
3. Hohmann, G. W., 1973, Electromagnetic coupling between grounded wires at the surface of a two-layer earth: *Geophysics*, v. 38, p. 854-863.
4. Kulikov A.V. et al. Technological recommendation on application of instruments for amplitude – phase low-frequency EM prospecting. Moscow, *Neftegeofizika*, 1985.
5. Matushko Ju.V. VES and IP-VES data interpretation at MSU training base "Alexandrovka". *Unpublished M. Sc. Thesis*, MSU, Moscow, 1997.
6. Millett, F. B., 1967, Electromagnetic coupling of collinear dipoles on a uniform half-space, in *Mining geophysics*, Vol. 2, SEG, Tulsa, pp. 401-419.
7. Nahabtcev A.S., Sapognikov B.G., Jabluchansky A.I. Electrical profiling with non-grounded working lines. Leningrad, 1985, 96 pp. (In Russian).
8. Sapozhnikov, B.G., 1996: Resistivity method without grounding. 21st General Assembly of the EGS, The Hague, 6-10 May, 1996. *Annales Geophysical, Supplement of Volume 14*, 1996.
9. Vishnjakov A.E. Serial electrical resistivity instruments. *Nedra*, Leningrad, 1967.